On the Interpretation of MOS Impedance Data in Both Series and Parallel Circuit Topologies

E. Caruso[1,4], J. Lin[1], S. Monaghan[1], K. Cherkaoui[1], L. Floyd[1], F. Gity[1], P. Palestri[2], D. Esseni[2], L. Selmi[3], P. K. Hurley[1]

[1]Tyndall National Institute University College Cork, Cork, Ireland, email: paul.hurley@tyndall.ie [2]DPIA, University of Udine, Via delle Scienze 206, 33100, Udine, Italy , [3]DIEF, University of Modena and Reggio Emilia, Via P. Vivarelli 10/1, 41125, Modena, Italy, [4] Infineon Technologies Villach, Austria

Introduction: The *ac* impedance/admittance modulus (Z, Y) and phase angle (θ) of the MOS structure at a given voltage is typically represented via its frequency-dependent capacitive (C) and conductive (G) elements according to *either* a series *or* a parallel equivalent circuit. The resulting C (ω,V) and G (ω,V) data are used to characterize the basic MOS structure and its electrically active defect parameters [1]. The objective of this contribution is to investigate the impact and significance of using *both* series *and* parallel equivalent circuit representations for the case of an MOS system in inversion. Our study comprises a mathematical analysis of the equivalent circuit models, physics based impedance simulations and experimental data for Si and InGaAs MOS structures.

Equivalent Circuit Representations: Fig 1(a) shows a 3 element equivalent circuit for an MOS structure in inversion (neglecting border traps), and Fig 1(b) and (c) illustrate the corresponding 2 element parallel, and series representations, respectively. The C_P (ω), G_P (ω), C_S (ω), G_S (ω) expressions are also given, where C_{ox}, is the oxide capacitance, C_{SC} the semiconductor capacitance, and G_{SC} is the semiconductor conductance. It was recently shown that G_P/ω and $-dC_{S,P}/d\log_e(\omega)$ (≡ $-\omega dC_{S,P}/d\omega$) , when interpreted in the parallel mode, both exhibit a maximum value of equal magnitude at the transition frequency (f_m) [2]. This relationship is true for all bias regions of the MOS CV/GV response [3]. Simplified analytical expressions for the magnitude and frequency of the maximum and minimum of $G_{S,P}/\omega$ and $-\omega dC_{S,P}/d\omega$ are shown in **Figure 2**. The results obtained from the parallel equivalent circuit model shown in Figure 2(a), are also replicated from physics-based *ac* simulations and observed in experimental MOS structures in inversion [2, 3].

When the impedance of **Fig 1 (a)** is interpreted in a ***series C_s, G_s circuit,*** G_S/ω ***exhibits a minimum, not*** a maximum. Moreover, the maximum of $-\omega dC_S/d\omega$ does not occur at the same frequency as the minimum in G_S/ω. This is significant, as interpretation of the impedance (Z, θ) data in both the series and parallel mode yields five separate features in the minima/maxima of the $-\omega dC/d\omega$ and G/ω functions. The magnitude of the functions at the maxima/minima is determined uniquely by C_{OX} and C_{SC}, with G_{SC} only appearing in the frequency of the maxima/minima. Moreover, the minima in the G_S/ω only depend on the depletion capacitance in inversion. While the assumption that C_{SC} and G_{SC} are independent of frequency at the maxima is not strictly correct for the parallel model (and induces errors), the G_S/ω minima now occurs at a frequency where C_{SC} and G_{SC} are independent of frequency (confirmed by device simulation) and, as a consequence, the N_D can be evaluated before extracting the oxide capacitance, C_{OX}. This allows C_{OX} evaluation from the maximum of the $-\omega dC_S/d\omega$, or from either maxima of the parallel circuit.

Experimental Results and Simulations for Si and InGaAs MOS structures: The $-\omega dC_{P,S}/d\omega$ and $G_{P,S}/\omega$ for a Si MOS constructed from the 80ºC experimental data of [4] (to induce an otherwise negligible minority carrier response) are shown in **Fig. 3,** demonstrating the form expected of the $-\omega dC_P/d\omega$, G_P/ω $-\omega dC_S/d\omega$, G_S/ω functions. The figure also shows *ac* simulations [5, 6], including Fermi-Dirac statistics, multi-valley band structure with non-parabolic corrections and SRH generation/recombination. The value of the silicon doping concentration (from $G_S/\omega = 2C_{SC}$ minima) is determined as 4×10^{15} cm^{-3}, in line with the value quoted in [4]. With the silicon doping determined directly from the series mode G/ω minima, the values of C_{ox} and the minority carrier generation lifetime (τ_g) can be determined from the peak frequency and peak magnitude in the parallel model ($-\omega dC_P/d\omega$ and G_P/ω) and the frequency of the $-\omega dC/d\omega$ in the series mode, using *ac* device simulations. Moreover, the doping concentration expression obtained directly from the G/ω minima is confirmed as correct based on the simulated multi-frequency CV/GV response.

Experimental multi-frequency C_P-V and G_P-V responses measured for $Ni/Al_2O_3/n\text{-}In_{0.53}Ga_{0.47}As/InP$ stacks, [7], are shown in **Fig 4.** The experimental and simulated (without traps) $G_{S,P}/\omega$ and $-\omega dC_{S,P}/d\omega$ functions (**Fig. 5**) are in excellent agreement and yield C_{OX}=0.098 F/m^2 (consistent with TEM thickness of 6.3 nm and ε_{ox} of 7 for Al_2O_3), τ_g= 80 ps and N_D=4.6x10^{17} cm^{-3}. The doping concentration is in agreement with the average InGaAs doping N_D value measured by electrochemical CV [3]. It is noted that despite the presence of a high density of oxide (border) traps in the Al_2O_3 InGaAs MOS system [7], the simulated $-\omega dC_{S,P}/d\omega$ and $G_{S,P}/\omega$ functions, without oxide traps, are still in very good agreement with the experimental data, mainly because oxide traps distributed in space do not generate extra peaks in the $G_{S,P}/\omega$ or $-\omega dC_{S,P}/d\omega$ functions, as will be explained in detail in the full paper.

Conclusions: Due to minority carrier generation in the depleted region, a minimum appears in the G_S/ω versus ω plots in the inversion region. Moreover, the $-\omega dC_{S,P}/d\omega$ and $G_{S,P}/\omega$ versus ω plots provide 5 independent values for the magnitude and frequency of the maxima and minima points. Analytic expressions obtained from the equivalent circuit representation are replicated from physics-based *ac* simulations and by experimental results for a close to ideal Si MOS and a non-ideal InGaAs MOS structure. The analytic equations obtained in the series mode (Fig 2b) are confirmed by simulations and allow for a direct extraction of MOS structure parameters. The approach described is applicable to any MOS system where an inversion response is detected over the bias, frequency and temperature range of the measurements.

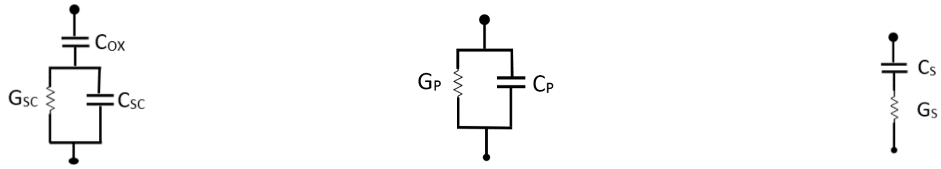

$Y = \frac{j\omega C_{ox}(G_{SC} + j\omega C_{SC})}{G_{SC} + j\omega(C_{ox} + C_{SC})}$	$C_p = C_{ox}\left[1 - \frac{\omega^2 C_{ox}(C_{ox} + C_{SC})}{G_{SC}{}^2 + (C_{ox} + C_{SC})^2\omega^2}\right]$ $G_p = \frac{\omega^2 C_{ox}{}^2 G_{SC}}{G_{SC}{}^2 + (C_{ox} + C_{SC})^2\omega^2}$	$C_S = \frac{C_{ox}(G_{SC}{}^2 + C_{SC}{}^2\omega^2)}{G_{SC}{}^2 + C_{SC}(C_{ox} + C_{SC})\omega^2}$ $G_S = G_{SC} + \frac{C_{SC}{}^2\omega^2}{G_{SC}}$

Figure 1. (a) The generic representation of the MOS system in inversion, (b) the parallel interpretation and corresponding G_P and C_P functions and (c), the series representation and the corresponding functions G_S and C_S functions.

Functions obtained from the equivalent circuit models

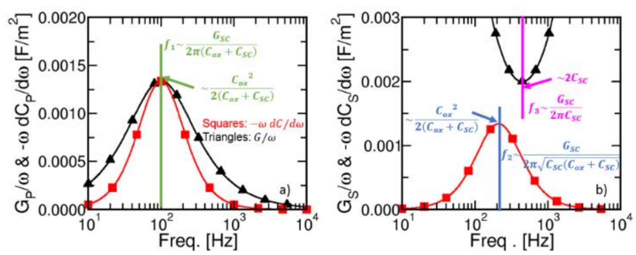

Figure 2: G/ω and -ωdC/dω functions obtained directly from the simplified analytic solutions of the **(a)** parallel and **(b)** series parallel RC networks. This example is for the case of an MOS structure with an oxide thickness T_{ox}=10 nm of relative permittivity 3.9, and a doping concentration of $N_D=5x10^{16}$ cm^{-3}. The transition frequency is selected as 100Hz which fixes G_{sc} = 2 S/m^2. The corresponding expressions for the maxima/minima and transition frequencies are shown inset in the figure, assuming G_{SC} and C_{SC} are frequency independent at the maxima/minima.

Experiments and simulations for a Si/SiO_2 MOS in inversion at 80°C, from [4]

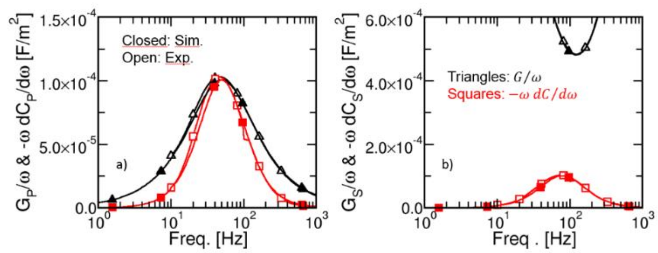

Figure 3. (a) G/ω and -ωdC/dω functions constructed from the experimental (open symbols) *n*-Si MOS data in inversion (V_G = -7V) [4], and **(b)** the corresponding series mode representation of the G/ω and -ωdC/dω functions. The experimental sample is 100nm SiO_2 on Si with nominal doping of $1x10^{15}$ cm^{-3}. The graph also show the device simulations at 80°C (closed symbols) indicating the same functional dependence as the experimental data, with precise matching obtained based on a silicon doping concentration of $4x10^{15}$ cm^{-3} and a silicon τ_g = 1ms.

Experimental C (ω,V) and G (ω,V) responses for an Al_2O_3/InGaAs MOS in inversion at 25°C, from [7]

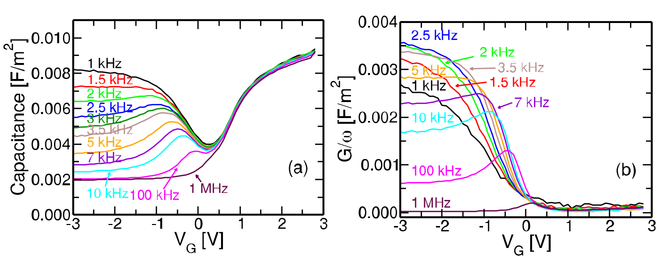

Figure 4. Experimental (a) C_P-V and (b) G_P-V responses at 25°C for an InGaAs MOS structure. (Ni/Al_2O_3 (6.3nm)/*n*-$In_{0.53}Ga_{0.47}As$/InP) [7]. Si n-type doping in the InGaAs layer is nominally $4x10^{17}cm^{-3}$. The gate leakage is negligible over the CV/GV bias range. The C (ω,V) and G (ω,V) responses shown are based on an interpretation of the measured (Z, θ) data in a parallel circuit mode.

Experimental (derived from figure 4) and simulations Al_2O_3/InGaAs MOS in inversion at 25°C, from [7]

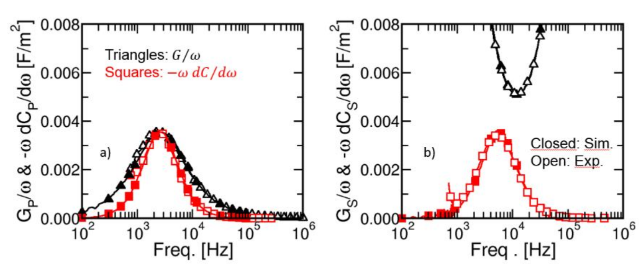

Figure 5. (a) G_P/ω and $-\omega dC_P/d\omega$ functions constructed from Fig.4 (V_G=-3V)**, (b)** corresponding series mode representation G_S/ω and $-\omega dC_S/d\omega$. Simulations (closed symbols) based on C_{OX}=0.098 F/m^2 τ_g= 80 ps and $N_D=4.6x10^{17}$ cm^{-3}. The simulations are in excellent agreement with the measured data for both circuit modes, and the doping concentration is in agreement with the value measured by electrochemical CV.

[1] E. H. Nicollian, J. R. Brews, Wiley, 1982 [2] S. Monaghan et al., DOI: 10.1109/TED.2014.2362524 [3] E. Caruso et al., DOI: 10.1109/SISPAD.2019.8870553 [4] G. Baccarani, et al., DOI: 10.1016/0038-1101(75)90177-X [5] S. E. Laux, DOI: 10.1109/T-ED.1985.22235. [6] Sentaurus Device Manual: L-2016.03-SP2 [7] E. Caruso *et al*., DOI: 10.1109/TED.2020.3018095. [8] Y. Yan *et al., IEEE EDL*, vol. 32, no. 4, p. 485, 2011